Elliptic flow of transported and produced protons in Au+Au collisions with the UrQMD model*

Biao Tu(涂彪) Shusu Shi(施梳苏)[1)] Feng Liu(刘峰)[2)]

Key Laboratory of Quarks and Lepton Physics (MOE) and Institute of Particle Physics, Central China Normal University, Wuhan, 430079, China

Abstract: Within the framework of the UrQMD model, by tracing the number of initial quarks in protons, we study the elliptic flow of protons with 3, 2, 1, 0 initial quarks and anti-protons in Au+Au collisions at $\sqrt{s_{\rm NN}}$ = 7.7, 11.5, 39, 200 GeV. The difference of elliptic flow between protons with 2, 1, 0 initial quarks and anti-protons is smaller than 0, or consistent with 0, respectively. The difference of elliptic flow between transported protons (with 3 initial quarks) and anti-protons is larger than 0 at 7.7, 11.5 and 39 GeV. This is in good agreement with the STAR results at 7.7 and 11.5 GeV, but overestimates the STAR results at 39 GeV. The yield of transported protons with 3 initial quarks is smaller than of protons with 2 and 1 initial quarks, and v_2 of all protons is much smaller than the STAR results. The observation of the difference of elliptic flow between transported protons and anti-protons in the UrQMD model partly explains the v_2 difference between protons and anti-protons observed in the Beam Energy Scan program at the Relativistic Heavy Ion Collider (RHIC).

Keywords: elliptic flow, UrQMD, beam energy scan

PACS: 25.75.Ld **DOI:** 10.1088/1674-1137/43/5/054106

1 Introduction

A strongly interacting hot and dense QCD matter called quark-gluon plasma (QGP) is created in the experiments with high-energy heavy-ion collisions at the Relativistic Heavy Ion Collider (RHIC) and the Large Hadron Collider (LHC) [1-6]. To understand the properties and phase structure of strongly interacting nuclear matter, the Beam Energy Scan (BES) program involving Au+Au collisions has been carried out at RHIC. Various observables have been measured such as the particle production ratios [7, 8], Hanbury-Brown-Twiss (HBT) terferometry [9], moments of the conserved quantities [10] and collective flow [11]. In this paper, we focus on the second harmonic of the collective flow, v_2. Analyzing the anisotropic flow in nucleus-nucleus collisions is one of the most important directions in studying the properties of created matter [12-14], since it is sensitive to the pressure gradient, degrees of freedom, equation of state (EoS) [15, 16] and degree of thermalization in the early stages of nuclear collisions.

Some interesting phenomena have been observed in heavy-ion collisions in the BES program. In particular, smaller v_2 for $\overline{p}$, K^- and π^+ than for p, K^+ and π^- were observed, and these v_2 differences decrease with increasing collision energy [17-21]. These interesting results were attributed to the different v_2 of transported and produced quarks during the initial stage of heavy-ion collisions in Ref. [22]. It is argued that this effect results from quark transport from forward to middle rapidity. The authors assume that v_2 of transported quarks is larger than of produced quarks. Thus, the different number of constituent quarks and anti-quarks in the particles and corresponding antiparticles leads to a systematically larger v_2 for baryons compared to anti-baryons. The energy dependence is explained by the increase of nuclear stopping in heavy-ion collisions with decreasing collision energy [23]. In Ref. [24], it is suggested that the chiral magnetic effect induced by the strong magnetic field in non-central collisions could be responsible for the observed difference between v_2 of π^+ and π^-.

A calculation [25, 26] based on the Nambu-Jona-Lasino(NJL) model can also qualitatively explain the differences between $p-\overline{p}$, $\Lambda-\overline{\Lambda}$ and K^+-K^- by incorport-

Received 19 November 2018, Revised 25 February 2019, Published online 18 March 2019

* Supported in part by the MoST of China 973-Project (2015CB856901), National Natural Science Foundation of China (11890711) and self-determined research funds of CCNU from the colleges' basic research and operation of MOE (CCNU18TS031)

1) E-mail: shiss@mail.ccnu.edu.cn

2) E-mail: fliu@mail.ccnu.edu.cn

ing a repulsive potential for quarks and attractive potential for antiquarks, which results in different flow patterns. Another study [27] , based on the AMPT model including mean-field potential, can also qualitatively explain the difference between the elliptic flow of particles and their corresponding antiparticles. Due to the stronger attractive potential for $\overline{p}$ compared to p, smaller v_2 is obtained for $\overline{p}$. With the attractive potential for K^- and repulsive for K^+ , and slightly attractive potential for π^+ and repulsive for π^- , smaller v_2 is obtained for K^- and π^+ than for K^+ and π^-.

In this paper, we study the elliptic flow of protons with 3, 2, 1 and 0 initial quarks and anti-protons at BES energies with the ultra relativistic quantum molecular dynamics (UrQMD) model [28, 29]. The paper is organized as follows: in Section 2, the observable is introduced. A brief description of the UrQMD model is given in Section 3. The results and discussion are presented in Section 4. Finally, a summary is given in Section 5.

2 Observable

The azimuthal anisotropy is one of the most important observables in heavy-ion collisions. In the non-central heavy-ion collisions, the overlap region is an almond shape with the major axis perpendicular to the reaction plane, which is defined by the impact parameter and the beam direction. As the system evolves, the pressure gradient from the overlapping region of two nuclei in the collision is at the origin of collective motion at mid-rapidity. The anisotropy in the coordinate space is transferred to the anisotropy in the momentum space. The anisotropic parameters are defined by the Fourier coefficients of the expansion of the azimuthal distribution [30, 31] of the produced particles with respect to the reaction plane, which can be written as

$$E\frac{\mathrm{d}^3N}{\mathrm{d}p^3}=\frac{1}{2\pi}\frac{\mathrm{d}^2N}{p_{\mathrm{T}}\mathrm{d}p_{\mathrm{T}}\mathrm{d}y}\left(1+2\sum v_n\cos[n(\phi-\Psi_{\mathrm{RP}})]\right), \quad (1)$$

where ϕ is the azimuthal angle of the particles. Ψ_{RP} is the reaction plane. The anisotropic parameter is defined as the n^{th} Fourier coefficient v_n:

$$v_n=\langle\cos[n(\phi-\Psi_{\mathrm{RP}})]\rangle, \quad (2)$$

where $\langle\cdots\rangle$ is the average over all the particles in the sample. The second harmonic coefficient is denoted as elliptic flow v_2. In the UrQMD model, Ψ_{RP} is fixed at zero degrees.

3 UrQMD model

The ultrarelativistic quantum molecular dynamics (UrQMD) model is a microscopic transport model which simulates p + p, p + A, and A + A collisions at relativistic energies, and describes the time-evolution of a many-body system using covariant equations of motion. It includes the string excitation and fragmentation, the formation and decay of hadronic resonances, and rescattering of hadrons. At low and intermediate energies, this microscopic transport model focuses on the interactions between known baryon and meson species and their resonances. The excitation and fragmentation of color strings play important roles in the particle production at high energies in the UrQMD model. The version of the UrQMD model we used in this study is 2.3, and no modification was made to the model itself, except for some additional output for tracing the particle origin as explained in ref. [32]. We marked particles as transported and produced by tracing the number of initial quarks in a particle. In this paper, protons with 3, 2, 1 and 0 initial quarks are marked as p (3 iq), p (2 iq), p (1 iq) and p (0 iq), respectively. There are two special cases. Protons with three initial quarks are treated as transported protons (p (3 iq)). Protons with zero initial quarks are treated as produced protons (p (0 iq)). Produced protons and anti-protons are both made of three produced quarks, thus they are expected to be similar in many aspects.

4 Results and discussion

By tracing the number of initial quarks in a proton, p (3 iq) accounts for 17.4% at 7.7 GeV, 8.3% at 11.5 GeV, 1.26% at 39 GeV and 0.36% at 200 GeV of all protons and anti-protons at mid- rapidity ($|Y|<1$). p (2 iq) accounts for 80.8% at 7.7 GeV, 84% at 11.5 GeV, 52.83% at 39 GeV and 10.9% at 200 GeV. p (1 iq) accounts for 0.91% at 7.7 GeV, 3% at 11.5 GeV, 12.46% at 39 GeV and 14.4% at 200 GeV. p (0 iq) accounts for 0.45% at 7.7 GeV, 2.4% at 11.5 GeV, 15.4% at 39 GeV and 39.1% at 200 GeV. $\overline{p}$ accounts for 0.44% at 7.7 GeV, 2.3% at 11.5 GeV, 18.05% at 39 GeV and 35.24% at 200 GeV. The upper panel of Fig. 1 shows the elliptic flow of p (3 iq), p (2 iq), p (1 iq), p (0 iq) and $\overline{p}$ within $0.2<p_{\mathrm{T}}<2.0$ GeV/c as a function of collision centrality in Au+Au collisions at various collision energies. One finds that v_2 shows strong centrality dependence, since it is mainly driven by the initial spatial eccentricity. The lower panel shows the difference of v_2 between p (3 iq), p (2 iq), p (1 iq), p (0 iq) and $\overline{p}$. The difference of v_2 between p (0 iq) (produced) and $\overline{p}$ does not clearly show the centrality dependence, and is approximately consistent with 0. As we mentioned above, p (0 iq) should be similar to $\overline{p}$ in many aspects, as they are both made of produced quarks. p (0 iq) and $\overline{p}$ are produced in the early stage of the system when the energy density is relatively large at low collision energies. Both p (0 iq) and $\overline{p}$ experience the full evolution of the system, which leads to a similar magnitude of v_2. Larger elliptic flow of p (3 iq) than of p (0 iq) or of $\overline{p}$ is observed. This

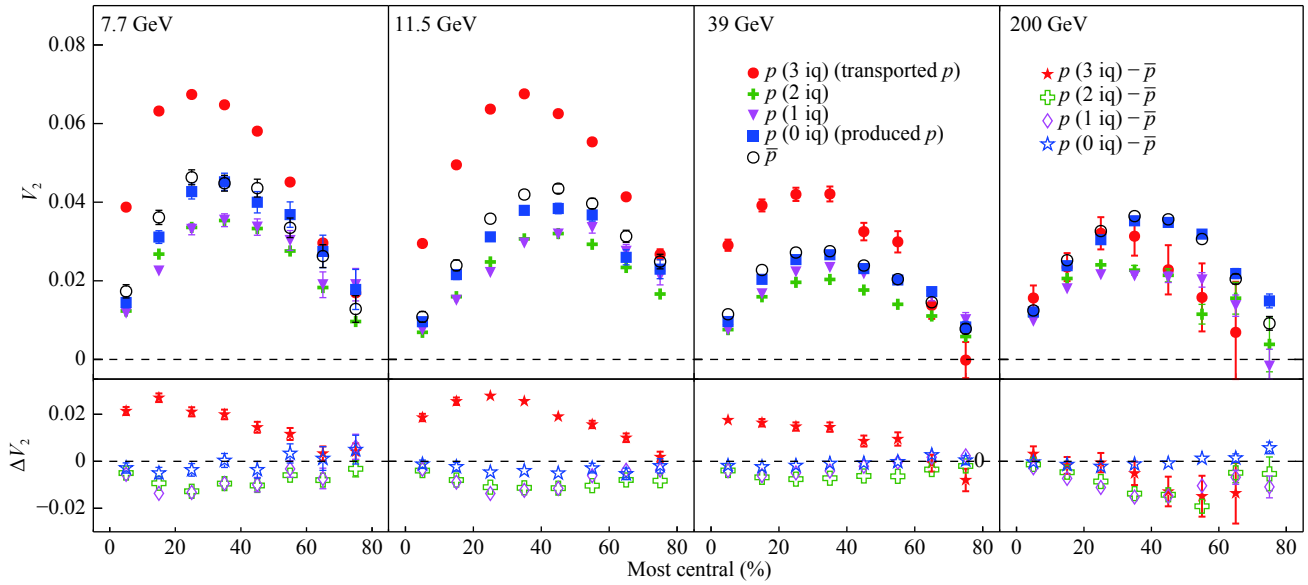

Fig. 1. (color online) Upper panel: The elliptic flow of p (3 iq), p (2 iq), p (1 iq), p (0 iq) and $\overline{p}$ are plotted as a function of collison centrality in Au+Au collisions at $\sqrt{s_{\rm NN}}$ = 7.7, 11.5, 39, 200 GeV. Lower panel: The difference of v_2 between p (3 iq), p (2 iq), p (1 iq), p (0 iq) and $\overline{p}$ as a function of collision centrality in Au+Au collisions at $\sqrt{s_{\rm NN}}$ = 7.7, 11.5, 39, 200 GeV.

suggests that v_2 of p (3 iq) derives from the transport from forward rapidity to mid-rapidity due to the nuclear stopping effect. The transported quarks, which are transported over a large rapidity, suffer more scatterings than produced quarks, which results in a larger v_2 , and leads to a larger v_2 of p (3 iq) than of p (0 iq). The difference ofv_2 between p (3 iq) and $\overline{p}$ shows a strong centrality dependence. A larger difference is observed in mid-central collisions than in most central and peripheral collisions at 7.7, 11.5 and 39 GeV. p (3 iq) experiences the whole process where the initial geometry eccentricity is transformed into anisotropy in the momentum space, whereas p (0 iq) may only partly experience this process. The combination of baryon stopping effect and scattering is the cause of the difference of v_2 between the transported protons and anti-protons, largest in mid-central collisions. No significant centrality dependence is observed at 200 GeV due to the small difference of v_2 between p (3 iq) and $\overline{p}$.

The elliptic flowv_2 of p (2 iq) and p (1 iq) show similar centrality dependence as v_2 of p (0 iq) and $\overline{p}$, but are systematically lower . p (0 iq), p (1 iq), p (2 iq) and $\overline{p}$ are produced at the same time in the early stage via the string excitation scheme [32], but part of p (1 iq) and p (2 iq) are produced in the decay of unstable baryons. This means that the formation time of p (0 iq) and $\overline{p}$ should be earlier than of p (1 iq) and p (2 iq). Hence, p (1 iq) and p (2 iq) suffer less interactions than p (0 iq) and $\overline{p}$. v_2 of p (1 iq) and p (2 iq) are smaller than of p (0 iq) and $\overline{p}$. Thus, in the UrQMD model, v_2 of the inclusive p is slightly lower than, or consistent with, v_2 of $\overline{p}$, depending on the collision energy, which is consistent with the results in ref [33].

The upper panel of Fig. 2 shows the elliptic flow of p (3 iq), p (2 iq), p (1 iq), p (0 iq) and $\overline{p}$ as a function of transverse momentum $p_{\rm T}$ in 0%-80% Au+Au collisions at $\sqrt{s_{\rm NN}}$ = 7.7, 11.5, 39, 200 GeV. The lower panel shows the difference of v_2 between p (3 iq), p (2 iq), p (1 iq), p (0 iq) and $\overline{p}$. The difference of v_2 between p (0 iq) and $\overline{p}$ does not show a clear $p_{\rm T}$ dependence, and is almost consistent with 0 , except at 7.7 GeV. However, the difference of v_2 between p (3 iq) and $\overline{p}$ shows a weak $p_{\rm T}$ dependence. The splitting of v_2 between p (3 iq) and p (0 iq) may be due to the stronger flow of transported quarks, which experience more interactions than produced quarks. This phenomenon is consistent with the study in ref [22], by assuming that v_2 of transported quarks is larger than of produced quarks, and results in a splitting of v_2 between protons and anti-protons. v_2 of p (2 iq) and p (1 iq) increase with $p_{\rm T}$, but are systematically smaller than of p (3 iq), p (0 iq) and $\overline{p}$.

In order to compare with the STAR results, we calculate the integrated elliptic flow v_2 of p (3 iq), p (2 iq), p (1 iq), p (0 iq) and $\overline{p}$ in the interval$0.2 < p_{\rm T} < 2.0$ GeV/c . In Fig. 3, panel (a) shows the integrated elliptic flow v_2 of p (3 iq), p (2 iq), p (1 iq), p (0 iq) and, panel (b) shows the difference in v_2 between the STAR measurements and the UrQMD model, as function of the collision energy in Au+Au collisions. v_2 of p (3 iq) is systematically larger than of p (0 iq) and $\overline{p}$. Thus, the v_2 difference between p (3 iq) and $\overline{p}$ is larger than 0. The v_2 difference between p (0 iq) and $\overline{p}$ is slightly smaller than 0, or consistent with 0, depending on the collision energy. v_2 of p (2 iq) and p (1 iq) are systematically smaller than of p (3 iq), p (0 iq) and $\overline{p}$. Therefore, the difference of v_2 between p (2 iq)/p

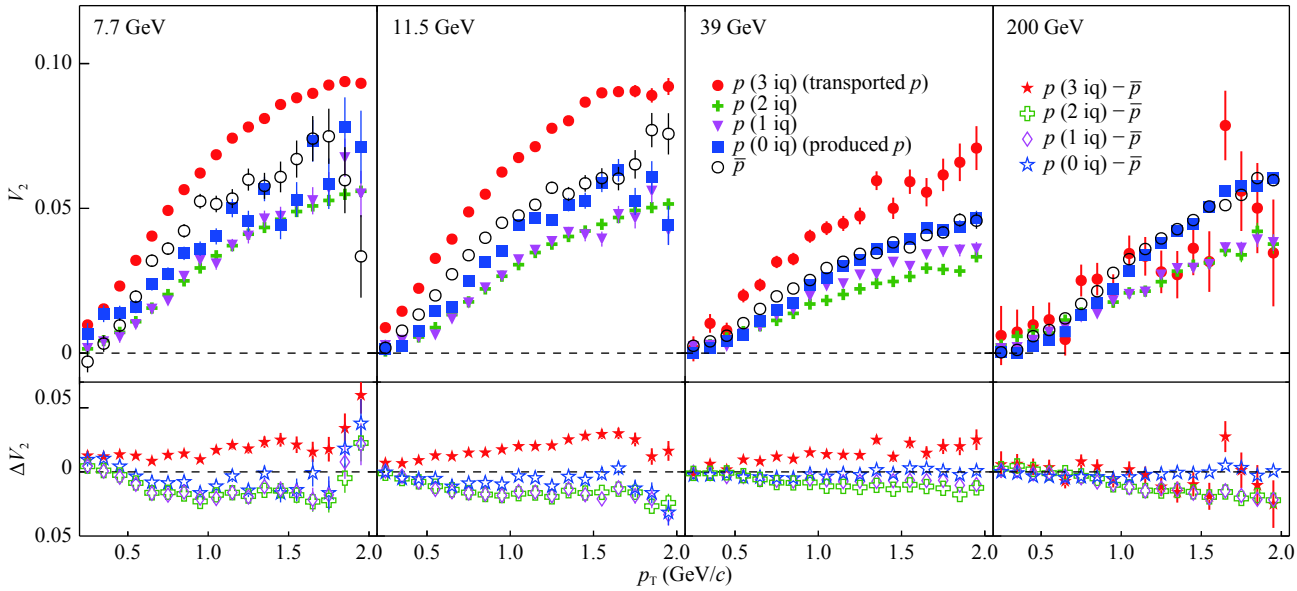

Fig. 2. (color online) Upper panel: The elliptic flow of p (3 iq), p (2 iq), p (1 iq), p (0 iq) and $\overline{p}$ as a function of the transverse momentum p_T for 0%-80% central Au+Au collisions at $\sqrt{s_{NN}}$ = 7.7, 11.5, 39, 200 GeV. The lower panels show the difference of $v_2(p_T)$ between p (3 iq), p (2 iq), p (1 iq), p (0 iq) and $\overline{p}$.

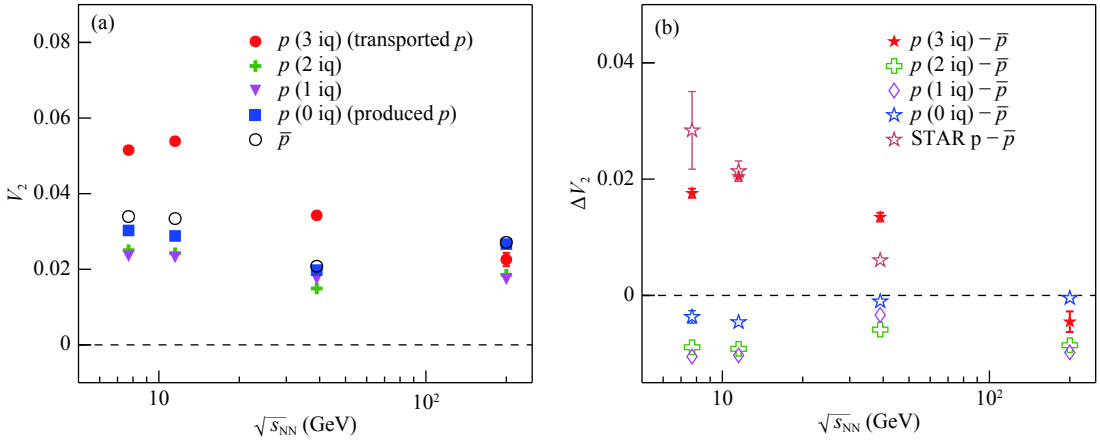

Fig. 3. (color online) Panel (a): The integrated v_2 of p (3 iq), p (2 iq), p (1 iq), p (0 iq) and $\overline{p}$ as a function of collision energy for 0%-80% central Au+Au collisions. Panel (b): The difference in v_2 between p (3 iq), p (2 iq), p (1 iq), p (0 iq) and $\overline{p}$ as a function of collision energy for 0%-80% central Au + Au collisions.

(1 iq) and $\overline{p}$ is smaller than 0. The difference of v_2 between p (3 iq) and $\overline{p}$ shows a similar energy dependence as the STAR results. Our results for p (3 iq) - $\overline{p}$ show good agreement with the STAR results below 11.5 GeV. At 39 GeV, the v_2 difference of p (3 iq) and $\overline{p}$ is not consistent with the STAR results quantitatively. The yield of p (3 iq) is relatively smaller than of p (2 iq) and p (1 iq), and v_2 of all protons is much smaller than the STAR result. This indicates that the v_2 difference with respect to STAR measurements may be partly due to the v_2 difference between p (3 iq) and $\overline{p}$. However, it can not explain the STAR results. In principle, the yield of p (3 iq) dominates the yield of protons at low energies. The magnitude of the v_2 difference p (3 iq) - $\overline{p}$, as the STAR data and the UrQMD model are consistent for Au+Au collisions at 7.7 and 11.5 GeV, suggests that the hadronic interactions are dominant at these collision energies. The v_2 difference between the STAR results and our calculations at 39 GeV indicates that the partonic interactions are also important for the increase of v_2 at high energies. Additionally, the fact that the fraction of p (3 iq) relative to inclusive protons decreases with increasing energy, can also lead to such a difference.

5 Summary

In summary, by tracing the number of initial quarks in

the UrQMD model, p (3 iq), p (2 iq), p (1 iq), p (0 iq) can be distinguished, which provides a way to study the elliptic flow of transported protons and produced protons. We found that the elliptic flow of produced protons shows similar dependence on collision centrality, transverse momentum and collision energy as of anti-protons. The possible explanation is that produced protons and anti-protons are both made of produced quarks. At the same time, the produced protons and anti-protons can only be produced at the early stage of the hadronic evolution of the system. Both experience similar magnitude of interactions in the system, which leads to similar v_2. For transported protons, the elliptic flow is systematically larger than for anti-protons as a function of collision centrality, transverse momentum and collision energy. This can be explained as following: quarks transported from forward rapidity to mid-rapidity by the baryon stopping effect gain larger v_2 than produced quarks. v_2 of p (2 iq) and p (1 iq) are systematically smaller than of transported protons, produced protons and anti-protons. Our results with the UrQMD model indicate that the splitting of v_2 for protons may partly arise from the difference of v_2 between transported quarks and produced quarks. The difference of v_2 between transported protons with 3 initial quarks and anti-protons shows good quantitative agreement with that between protons and anti-protons in the STAR measurements at low energies (7.7 and 11.5 GeV), but also large deviation at high energies ($\geqslant$ 39 GeV). This suggests that hadronic interactions are dominant in collisions at 7.7 and 11.5 GeV. Without partonic interactions in the UrQMD model, it is problematic to reproduce v_2 at high energies ($\geqslant$ 39 GeV). On the other hand, the fraction of transported protons relative to inclusive protons may also contribute to the difference between the STAR data and the UrQMD model.

References

1 I. Arsene et al (BRAHMS Collaboration), Nucl. Phys. A, **757**: 1 (2005)
2 B. B. Back et al (PHOBOS Collaboration), Nucl. Phys. A, **757**: 28 (2005)
3 J. Adams et al (STAR Collaboration), Nucl. Phys. A, **757**: 102 (2005)
4 K. Adcox et al (PHENIX Collaboration), Nucl. Phys. A, **757**: 184 (2005)
5 K. Aamodt et al (ALICE Collaboration), Phys. Rev. Lett., **105**: 252302 (2010)
6 K. Aamodt et al (ALICE Collaboration), Phys. Rev. Lett., **106**: 032301 (2011)
7 Z. Q. Feng, Nucl. Sci. Tech., **29**: 40 (2018)
8 X. H. Jin, J. H. Chen, Y. G. Ma, S. Zhang, C. J. Zhang, and C. Zhong, Nucl. Sci. Tech., **29**: 54 (2018)
9 J. Yang and W. N. Zhang, Nucl. Sci. Tech., **27**: 147 (2016)
10 X. Luo and N. Xu, Nucl. Sci. Tech., **28**: 112 (2017)
11 H. Song, Y. Zhou, and K. Gajdosova, Nucl. Sci. Tech., **28**: 99 (2017)
12 J. Y. Ollitrault, Phys. Rev. D, **46**: 229 (1992)
13 H. Sorge, Phys. Rev. Lett., **78**: 2309 (1997)
14 H. Sorge, Phys. Rev. Lett., **82**: 2048 (1999)
15 C. M. Ko and F. Li, Nucl. Sci. Tech., **27**(6): 140 (2016)
16 Z. Y. Lu, G. X. Peng, S. P. Zhang, M. Ruggieri, and V. Greco, Nucl. Sci. Tech., **27**: 148 (2016)
17 L. Adamczyk et al (STAR Collaboration), Phys. Rev. Lett., **110**(14): 142301 (2013)
18 L. Adamczyk et al (STAR Collaboration), Phys. Rev. C, **88**: 014902 (2013)
19 L. Adamczyk et al (STAR Collaboration), Phys. Rev. C, **86**: 054908 (2012)
20 L. Adamczyk et al (STAR Collaboration), Phys. Rev. C, **93**: 014907 (2016)
21 Shusu Shi, Adv. High Energy Phys., **2016**: 1987432 (2016)
22 J. C. Dunlop, M. A. Lisa, and P. Sorensen, Phys. Rev. C, **84**: 044914 (2011)
23 P. C. Li, Y. J. Wang, Q. F. Li, and H. F. Zhang, Nucl. Sci. Tech., **29**: 177 (2018)
24 Y. Burnier, D. E. Kharzeev, J. Liao, and H. U. Yee, Phys. Rev. Lett., **107**: 052303 (2011)
25 J. Xu, T. Song, C. M. Ko, and F. Li, Phys. Rev. Lett., **112**: 012301 (2014)
26 C. M. Ko, T. Song, F. Li, V. Greco, and S. Plumari, Nucl. Phys. A, **928**: 234 (2014)
27 J. Xu, L. W. Chen, C. M. Ko, and Z. W. Lin, Phys. Rev. C, **85**: 041901 (2012)
28 M. Bleicher et al, J. Phys. G, **25**: 1859 (1999)
29 S. A. Bass et al, Prog. Part. Nucl. Phys., **41**: 255 (1998)
30 S. Voloshin and Y. Zhang, Z. Phys. C, **70**: 665 (1996)
31 A. M. Poskanzer and S. A. Voloshin, Phys. Rev. C, **58**: 1671 (1998)
32 Y. Guo, F. Liu, and A. Tang, Phys. Rev. C, **86**: 044901 (2012)
33 Q. Li, Y. Wang, X. Wang, and C. Shen, Sci. China Phys. Mech. Astron., **59**: 632001 (2016)